DOI: 10.1002/((please add manuscript number))
Article type: Communication

Click-Chemistry Immobilized 3D-infused Microarrays in Nanoporous Polymer Substrates

Michael Hirtz, Wenqian Feng, Harald Fuchs, and Pavel A. Levkin**

Dr. M. Hirtz, Prof. H. Fuchs
Institute of Nanotechnology (INT) and Karlsruhe Nano Micro Facility (KNMF), Karlsruhe Institute of Technology (KIT), Germany
E-mail: michael.hirtz@kit.edu

W. Feng, Dr. P. A. Levkin
Institute of Toxicology and Genetics (ITG), Karlsruhe Institute of Technology (KIT), Germany
E-mail: pavel.levkin@kit.edu

Prof. H. Fuchs
Physical Institute and Center for Nanotechnology (CeNTech), University of Münster, Germany

Dr. P. A. Levkin
Applied Physical Chemistry, Heidelberg University, Germany

Keywords: 3D microarrays, click-chemistry, microspotting, CuAAC, polymer films

Microarrays are widely used in many fields of biological and biomedical research as well as in medical diagnostics.[1–6] For reliable use, the microarrays should be stable, homogeneous and easy to read out, while at the same time, miniaturizing is desired for reduced use of consumables and sample. Recently, we have shown the advantageous properties of nanoporous HEMA-EDMA polymer for the generation of miniaturized microarrays in comparison to conventional spotting substrates.[7] The microarrays fabricated on the nanoporous HEMA-EDMA polymer could feature smaller spot sizes (at least one order of magnitude less than in typical ink jet printing) while retaining sharper feature edges when compared to other commonly used substrates for spotting as paper, nitrocellulose and nylon membranes. This higher pattern fidelity allows for the reduction of spot size, while still obtaining well-defined features, thus facilitating readout of the arrays and saving materials. However, a substrate with similar properties but functionality for covalent binding of spotted substances would be of great importance to many applications in spotting and sensing, nanostructured surfaces being e.g. used for enhanced capture and detection of bacteria.[8] Alkyne modification of glass substrates[9] allowed for the formation of covalently bound microarrays by spotting with molecules functionalized with the azide group.[10] To combine the favorable properties of the nanoporous polymeric substrates (average pore size 150 nm)[7] with the covalent binding demonstrated on the glass substrates, we here present an alkyne modification of the porous polymer (alkyne-HEMA-EMDA) allowing for click-chemistry coupling of azides via copper(I)-catalyzed azide-alkyne cycloaddition (CuAAC).[11–13] This prominent click reaction found many applications, e.g. in the generation of nanosized molecular junctions.[14] The polymer retains its desirable spotting properties and covalently immobilized high quality microarrays can be generated. The three dimensional impregnation of the polymer with a fluorescently labeled azide is quantified by confocal microscopy and leads to considerably higher spot fluorescence intensities compared to strictly 2-dimensional surfaces as modified glass. Furthermore, the microarrays can be multiplexed and used for

binding of proteins, as is demonstrated by selective binding of streptavidin and specific antibody on an allergen array.

Figure 1a shows the schematic spotting setup as used in the present work. A quill-like microchannel cantilevers, called surface patterning tools (SPTs)[15] is brought into contact with the alkyne-HEMA-EMDA surface for defined time lengths allowing the imbibition of spotting solution into the polymer. By high precision scanning in x- and y- direction via the stage of a dip-pen nanolithography (DPN) platform (NLP 2000, NanoInk, USA), the spot features of the microarray are generated one after the other. The spotting solution is based on water with admixing of glycerol to prevent drying out. It contains an azide-modified molecule for immobilization, sodium ascorbate and copper sulfate to catalyze the CuAAC reaction. The chemical structure of the used azides is given in Figure 1b for tetramethylrhodamine (TAMRA) azide and Figure 1c for biotin azide, respectively.

A typical outcome of a spotting with TAMRA azide is shown in **Figure 2a**. This pattern of 100 spots arranged in a square with a pitch of 50 μm (yielding an array area of 500 × 500 μm²) was written with a dwell time of 0.5 s by a single quill-like pen in about one minute. Generally, the spotting procedure can be parallelized by introduction of pen arrays,[16] yielding even higher throughput with larger areas and additional possibility of intrinsic multiplexing. In our present setup, we realized multiplexing by subsequent writing with tip changing for the different inks, which could principally automated as alternative route to multiplexed arrays. Due to the CuAAC mediated covalent immobilization of desired molecules the pattern becomes highly stable in solution (see Supporting Information, **Figure S1** and **Figure S2**). The average radius of a dot feature in such arrays is (9.9 ± 0.5) μm, a histogram of the radius distribution is given in Figure 2f. To demonstrate the three-dimensional structure of the generated patterns due to imbibition of ink into the three dimensional porous polymer layer, we employed confocal microscopy. A 3D representation of a typical array as obtained from

confocal microscopy is shown in Figure 2b with a cross-section through one row of dots shown in Figure 2c. The outlines of the dot features as obtained by a thresholding of fluorescent intensity are added to the section and from this the hemispherical shape of the deposited dot features within the polymer film becomes obvious. To characterize the ink transport process during lithography, dot patterns with varying dwell times were spotted (Figure 2e). The radius of the dot features increases from about 8 μm up to 14 μm with increasing dwell time from 0.1 s to 2.0 s (Figure 2g). For imbibition of a fluid into a porous substrate, theory predicts a dependence on time proportional to $t^{1/3}$.[17] The spot radius vs. dwell time dependence in our system follows this prediction, deviating only for smaller dwell times especially in the case of 0.1 s (smallest dwell time possible in our setup). This could be an artifact introduced by a combination of the DPN system used contacting the surface some time longer then intended for this small dwell times near the system's limit and the deviation of our SPT (which has an opening at the apex of about 1 μm) from a point source as assumed in the theoretical description. Figure 2d contains a section through one row of the dot array in Figure 2e and shows that also the functionalized volume within the polymer film is dependent on dwell time as expected. With the radius r being proportional to $t^{1/3}$ it is expected that the volume V of functionalized polymer (being a half sphere) should be direct proportional to t. Plotting of the dot feature volume against dwell time (Figure 2h) reveals that our system exhibits a linear dependence on dwell time. Likewise to the radius, even at short dwell time the deposited volume does not reach zero, again reflecting a minimum volume of ink transfer just by touching the surface with a SPT. The volume character of the microarray features leads to a strong increase in fluorescence intensity compared to the strictly 2D nature of the features on glass slides. In the TAMRA-azide spots a 20-fold increase in signal intensity could be observed (**Figure S3**).

To demonstrate the capability of the approach for multiplexing and the stability of the microarrays for analyte binding from solution, we created bi-color patterns with alternating TAMRA-azide and biotin-azide spots. This was done by writing TAMRA-azide spots as described above, but leaving each second spot free and then subsequently filling these empty spaces with biotin-azide spots after replacing of the SPT. Biotin can serve as a strong binding motive for streptavidin,[18] effectively immobilizing the protein onto the biotin-azide functionalized spots in the array (**Figure 3a**). Since the biotin-azide is not fluorescent, only the TAMRA-azide spots are visible in fluorescent images of the array prior to fluorescently labeled streptavidin binding (Figure 3b). After incubation of the microarray with a solution containing fluorescein conjugated streptavidin, the prior invisible biotin-azide spots light up in the green channel of the fluorescent imaging indicating successful and selective binding of the protein.

To further elucidate the prospects of the polymer coating based microarrays for sensing and binding of biological relevant proteins, we compared the binding of antibodies to antigen-arrays on glass slides and alkyne-HEMA-EDMA polymer substrates (**Figure 4**). Glass was chosen as comparison for its broad use in similar assays, and to clearly contrast the 3D infused arrays to purely 2D ones (no diffusion in or swelling of substrate). For this experiment, microarrays of dinitrophenol (DNP)-azide were patterned on alkyne modified glass and alkyne-HEMA-EDMA substrates as described above. DNP can act – among other uses[19] - as a model allergen for the activation of mast cells,[20–23] here we use it as target for specific antibody binding.[24,25] After spotting and washing of the samples, solutions with different concentrations of fluorescently labelled anti-DNP antibodies (starting from 10 μg/ml in the highest concentration and then diluted 1:1 by volume with PBS for each following dilution step). Figure 4a shows a typical outcome of such antibody binding to a DNP microarray on an alkyne-HEMA-EDMA sample, showing clearly preferential binding of the

antibody to the DNP features of the array. Quantifying the resulting fluorescence signals for the series of antibody dilutions on alkynized HEMA-EDMA and comparison with the analog experiment on glass substrate samples further validates the discussed feature volume effect (Figure 4b): while for low antibody concentrations (0.125 and 0.250 relative antibody concentration) both substrate systems behave similar, the signal on the glass substrate levels off, while on alkyne-HEMA-EDMA substantially higher intensities are found for increasing antibody concentration (0.500 and 1.000 relative concentration). This behavior indicates, that the accessible binding sites (i.e. DNP moieties) on the glass slide are already completely saturated on the glass slide at the 0.250 relative antibody concentration. Therefore, further increase in antibody concentration cannot result in an increased fluorescence signal. On the alkyne-HEMA-EDMA substrate, additional binding sites are available in the bulk volume of the feature, hence enabling further increase in binding and fluorescence intensity on higher relative concentrations.

In conclusion, we present a novel platform for the immobilization of azide functionalized compounds and subsequently protein binding. The use of quill-like pens enables the delivery of higher ink volumes than e.g. microcontact printing or similar methods, therefore allowing infiltration into the porous substrate. This gives increased intensity from fluorescent compounds since the whole functionalized volume can contribute to the signal. Additionally, the method allows for multiplexed arrays with different compounds within one array. The micropatterns show high stability under immersion in solvents and can be used for selective binding of proteins as e.g. streptavidin or antibodies. The volume nature of the microarray features on alkyne-HEMA-EDMA substrate allows for additional binding sites when using the arrays as protein targets, resulting in a higher dynamic range of quantifiable concentrations when compared to 2D microarrays on non-porous substrates. While the porous nature of the functionalized volume limits the access by liquid exchange and diffusion speed

to this additional sensitive area, the higher dynamic range gained enables testing of a much wider range of target concentrations, allowing easier application of such assays. As the overall size of pores is in the range of 150 nm, this sets an upper limit of target size, though typical protein targets will be not inflicted, as they are much smaller. Overall, these properties make the presented porous polymer film an attractive substrate for microarraying e.g. for bio-medical or environmental testing.

Experimental Section

Substrate preparation: The fabrication of alkyne-HEMA-EDMA polymer film was described in our previous work.[26] Briefly, a 12.5 μm thin, hydrophilic porous polymer film was firstly prepared on a glass substrate using photoinitiated copolymerization of 2-hydroxyethyl methacrylate and ethylene dimethacrylate in the presence of porogens (non-alkynized HEMA-EDMA).[27] This procedure leads to the formation of a thin film of a highly cross-linked and porous (due to the presence of porogens) polymethacrylate layer. The porous structure is permeable network of interconnected polymer nanoglobules with pores of around 150 nm. The polymer surface was esterified by immersing into a dichloromethane solution containing 4-pentynoic acid (22.8 mM), coupling reagent *N,N'*-diisopropylcarbodiimide (22.8 mM), and catalyst 4-(dimethylamino)pyridine (9.2 mM) and stirring at RT for 4 h. A porous HEMA-EDMA layer functionalized with alkyne groups (alkyne-HEMA-EDMA) was produced.

Spotting Setup: The spotting procedures were done on a NLP 2000 system (NanoInk, USA) equipped with SPT pens (SPT-S-C10S, Bioforce Nanosciences). Prior to use, the SPTs were freshly plasma cleaned by oxygen plasma (10 sccm O2, 100 mTorr, 30 W for 2 min) and used immediately. The SPT was mounted onto the tip holder by double-sided sticky tape, and the pen reservoir was filled with 1 μL of azide solution. All spotting procedures were implemented at a relative humidity of 60% and with the sample stage tilted by 8° with respect to the SPT tip to minimize the chance of contact between the ink reservoir and the sample

surface. For all patterns, except for the pattern used for spot size versus dwell time analysis, a dwell time of 0.5 s was used.

Streptavidin binding: After the spotting process, the samples were washed extensively with DI water (18.2 MΩcm) to remove excess ink. Prior to adding the streptavidin solution, samples were blocked with 5% bovine serum albumin (BSA)[28] (Sigma-Aldrich) in phosphate buffered saline (PBS) (Gibco) for 10 minutes. Subsequently, the samples were washed 3 times by pipetting on and off 100 µl of PBS (3 times each) and then incubated for 10 minutes with a solution of 5 µg/ml of streptavidin fluorescein conjugate (Calbiochem/Merck). After repeating the washing steps, samples were imaged with fluorescence microscopy.

Antibody Binding: Microarrays of DNP-azide were generated on alkyne-HEMA-EMDA and glass substrates (glass substrates alkyne modification was performed as described in the literature)[9,10] as described above and washed with DI water (18.2 MΩcm) to remove excess ink. Then, the samples were blocked with 5% BSA (Sigma-Aldrich) in PBS (Gibco) for 10 minutes. Subsequently, the samples were washed 3 times by pipetting on and off 100 µl of PBS (3 times each) and then incubated with different concentrations of mouse anti-DNP antibody previously fluorescently labelled by a Mix-n-Stain CF 488A antibody labelling kit (both Sigma-Aldrich, Germany) for 60 minutes. The highest concentration of antibody was 10 µg/ml and more and more diluted solutions were created by admixing the previous solution 1:1 by volume with PBS, resulting in relative concentrations of 0.500, 0.250, and 0.125, respectively, compared to the highest concentration. After incubation, the samples were washed 3 times again and then imaged by fluorescence microscopy.

Imaging setup: Fluorescent microscopic images were obtained on an Eclipse 80i upright fluorescence microscope (Nikon) equipped with an Intensilight (Nikon) for illumination and a

CoolSNAP HQ2 camera (Photometrics). The confocal images were recorded using a Leica TCS SP5 confocal microscope.

Image analysis: The fluorescent microscopy images used for the determination of size distribution and influence of dwell time were analysed with ImageJ.[29,30] After converting the images to black and white by a threshold filter, the spot sizes were obtained by particle analyses. Particles smaller than 20 pixels were excluded from analysis to exclude noise-induced artefacts. To determine the functionalized polymer volume from the confocal images, this procedure was applied to each layer of the image stack, the resulting areas multiplied with the thickness of one layer and associated volume slices for each point were summed up.

Supporting Information

Supporting Information is available from the Wiley Online Library or from the author.

Acknowledgements

This work was carried out with the support of the Karlsruhe Nano Micro Facility (KNMF, www.kmf.kit.edu), a Helmholtz Research Infrastructure at Karlsruhe Institute of Technology (KIT, www.kit.edu). The research is supported by the ERC Starting Grant (ID: 337077-DropCellArray) and the Helmholtz Association's Initiative and Networking Fund (grant VH-NG-621).

Received: ((will be filled in by the editorial staff))
Revised: ((will be filled in by the editorial staff))
Published online: ((will be filled in by the editorial staff))

[1] V. Romanov, S. N. Davidoff, A. R. Miles, D. W. Grainger, B. K. Gale, B. D. Brooks, *Analyst* **2014**, *139*, 1303–26.

[2] M. B. Miller, Y. W. Tang, *Clin. Microbiol. Rev.* **2009**, *22*, 611–633.

[3] J. M. Lucas, *Allergol. Immunopathol. (Madr).* **2010**, *38*, 217–23.

[4] J. M. Lucas, *Allergol. Immunopathol. (Madr).* **2010**, *38*, 153–61.

[5] Z. He, Ed. , *Microarrays: Current Technology, Innovations and Applications*, Caister Academic Press, **2014**.

[6] H. Chandra, P. J. Reddy, S. Srivastava, *Expert Rev. Proteomics* **2011**, *8*, 61–79.

[7] M. Hirtz, M. Lyon, W. Feng, A. E. Holmes, H. Fuchs, P. A. Levkin, *Beilstein J. Nanotechnol.* **2013**, *4*, 377–384.

[8] Y.-Q. Li, B. Zhu, Y. Li, W. R. Leow, R. Goh, B. Ma, E. Fong, M. Tang, X. Chen, *Angew. Chemie Int. Ed.* **2014**, *53*, 5837–5841.

[9] S. Oberhansl, M. Hirtz, A. Lagunas, R. Eritja, E. Martinez, H. Fuchs, J. Samitier, *Small* **2012**, *8*, 541–545.

[10] M. Hirtz, A. M. Greiner, T. Landmann, M. Bastmeyer, H. Fuchs, *Adv. Mater. Interfaces* **2014**, *1*, 1300129.

[11] V. V Rostovtsev, L. G. Green, V. V Fokin, K. B. Sharpless, *Angew. Chemie Int. Ed.* **2002**, *41*, 2596–9.

[12] C. W. Tornøe, C. Christensen, M. Meldal, *J. Org. Chem.* **2002**, *67*, 3057–64.

[13] L. Liang, D. Astruc, *Coord. Chem. Rev.* **2011**, *255*, 2933–2945.

[14] X. Chen, A. B. Braunschweig, M. J. Wiester, S. Yeganeh, M. A. Ratner, C. A. Mirkin, *Angew. Chemie Int. Ed.* **2009**, *48*, 5178–5181.

[15] J. Xu, M. Lynch, J. L. Huff, C. Mosher, S. Vengasandra, G. Ding, E. Henderson, *Biomed. Microdevices* **2004**, *6*, 117–23.

[16] J. Xu, M. Lynch, S. Nettikadan, C. Mosher, S. Vegasandra, E. Henderson, *Sensors Actuators B Chem.* **2006**, *113*, 1034–1041.

[17] J. Xiao, H. A. Stone, D. Attinger, *Langmuir* **2012**, *28*, 4208–12.

[18] N. M. Green, *Adv. Protein Chem.* **1975**, *29*, 85–133.

[19] H. C. H. Lee, C. Y. Law, M. L. Chen, Y. H. Lam, A. Y. W. Chan, T. W. L. Mak, *J. Chinese Med. Assoc.* **2014**, *77*, 443–445.

[20] R. N. Orth, M. Wu, D. A. Holowka, H. G. Craighead, B. A. Baird, *Langmuir* **2003**, *19*, 1599–1605.

[21] S. Sekula-Neuner, J. Maier, E. Oppong, A. C. B. Cato, M. Hirtz, H. Fuchs, *Small* **2012**, *8*, 585–591.

[22] E. Oppong, P. N. Hedde, S. Sekula-Neuner, L. Yang, F. Brinkmann, R. M. Dörlich, M. Hirtz, H. Fuchs, G. U. Nienhaus, A. C. B. Cato, *Small* **2014**, *10*, 1991–1998.

[23] D. Jiang, J. Ji, L. An, X. Sun, Y. Zhang, G. Zhang, L. Tang, *Biosens. Bioelectron.* **2013**, *50*, 150–156.

[24] C. A. J. Janeway, P. Travers, M. Walport, M. J. Shlomchik, *Immunobiology*, Garland Science, New York, **2001**.

[25] G. W. Litman, J. P. Rast, M. J. Shamblott, R. N. Haire, M. Hulst, W. Roess, R. T. Litman, K. R. Hinds-Frey, A. Zilch, C. T. Amemiya, *Mol. Biol. Evol.* **1993**, *10*, 60–72.

[26] W. Feng, L. Li, E. Ueda, J. Li, S. Heißler, A. Welle, O. Trapp, P. a. Levkin, *Adv. Mater. Interfaces* **2014**, *1*, 1400269.

[27] F. L. Geyer, E. Ueda, U. Liebel, N. Grau, P. A. Levkin, *Angew. Chemie Int. Ed.* **2011**, *50*, 8424–7.

[28] H. Schønheyder, P. Andersen, *J. Immunol. Methods* **1984**, *72*, 251–9.

[29] M. D. Abràmoff, P. J. Magalhães, S. J. Ram, *Biophotonics Int.* **2004**, *11*, 36–42.

[30] C. A. Schneider, W. S. Rasband, K. W. Eliceiri, *Nat. Methods* **2012**, *9*, 671–675.

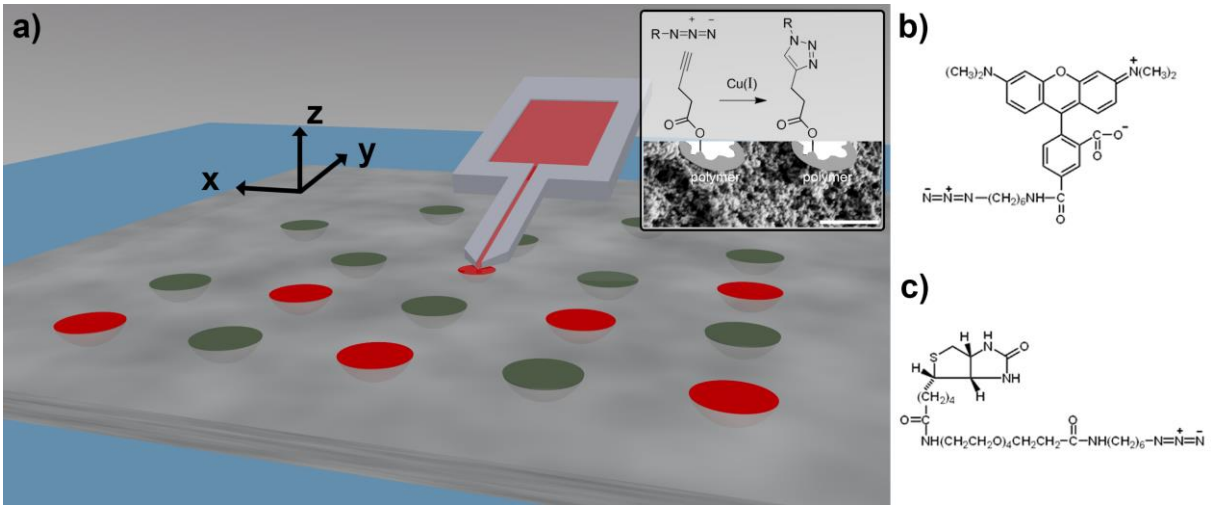

Figure 1. (a) Schematic view of the patterning process on the porous polymers. The inset shows the CuAAC reaction taking place on the alkyne-HEMA-EMDA substrate. Structures of the azides that were immobilized are shown in (b) for TAMRA azide and (c) for biotin azide.

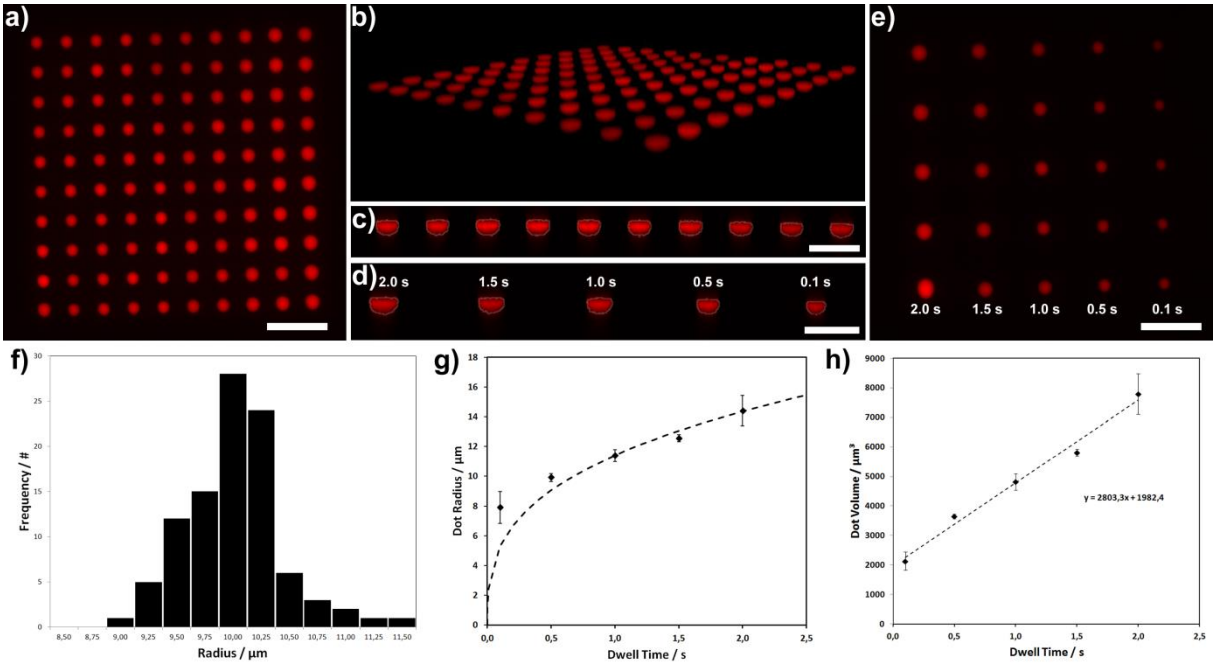

Figure 2. (a) Fluorescent microscopy image of a pattern TAMRA azide dot array. Scale bar equals 100 µm. (b) 3D image of a 10 × 10 dot array obtained with confocal microscopy to determine the volume distribution of the TAMRA azide within the polymer film. (c) Section through a line of dots from (b). Scale bar equals 50 µm, dot volume is outlined. (d) Section through a line of dots from (e) written with different dwell times. Scale bar equals 50 µm, dot volume is outlined. (e) 5 × 5 dot array with columns written with different dwell times. Scale bar equals 100 µm. (f) Histogram of the radius distribution of 100 dot features written at a dwell time of 0.5 s. (g) Dependence of the dot radius on dwell time. The dashed line follow $r = 11.4\ t^{1/3}$. (h) Dependence of dot volume on dwell time. The dashed line follows $r = 2803.3\ t + 1982.4$.

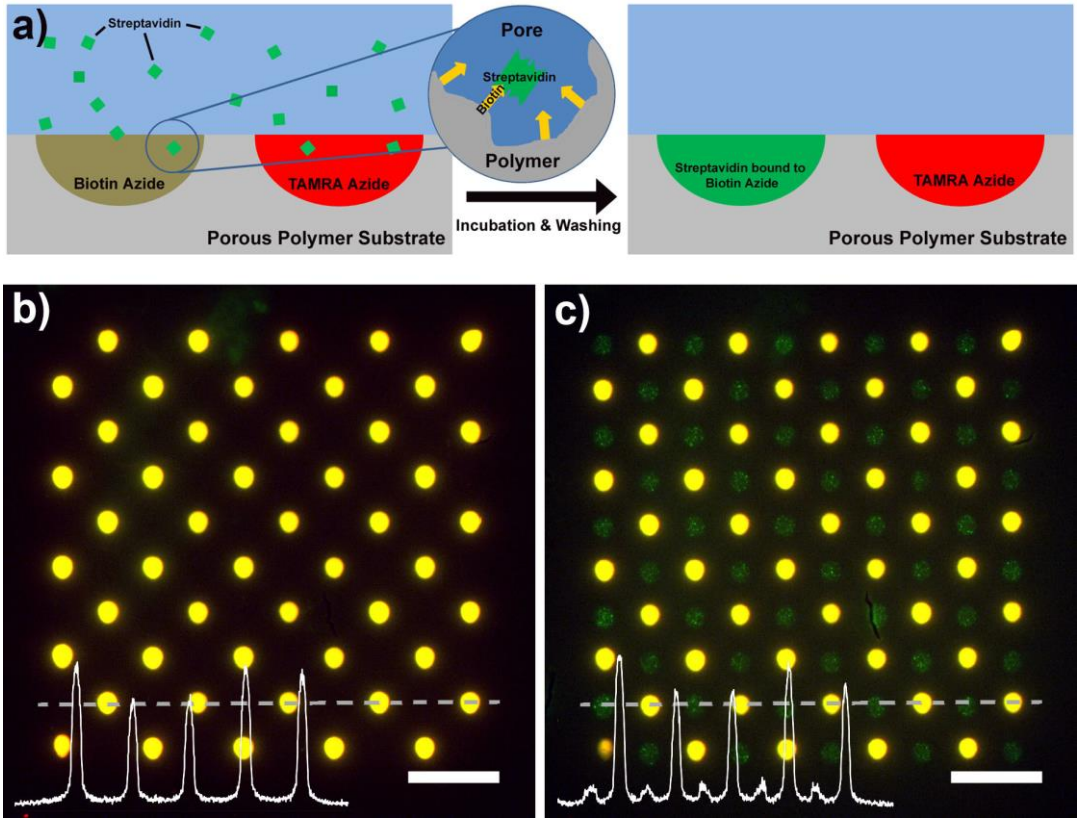

Figure 3. (a) Scheme of binding of streptavidin to multiplexed biotin- / TAMRA-azide microarrays. (b) Fluorescent microscopy image (green and red channel combined) of a multiplexed biotin- / TAMRA-azide microarray after washing. Only the TAMRA containing spots are visible. (c) Same microarray after incubation with fluorescein conjugated streptavidin. Now the previously invisible biotin-azide spots light up in the green channel. All scale bars equal 100 µm. The insets in the lower left of (b) and (c) show fluorescence intensity along the dashed lines.

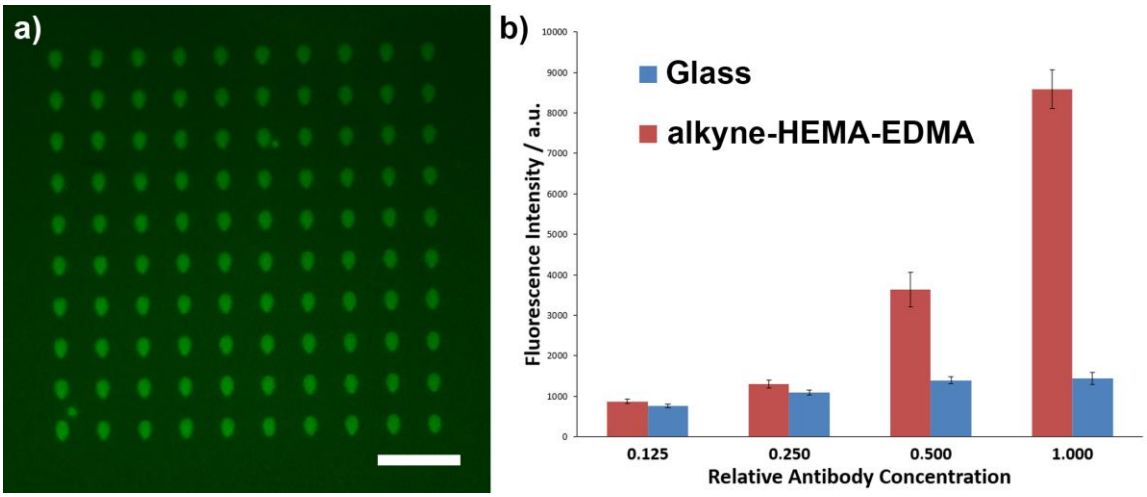

Figure 4. (a) Fluorescence microscopy image of a DNP-azide microarray on an alkynized HEMA-EDMA substrate after incubation with fluorescently labelled anti-DNP-antibody. Scale bar equals 100 µm. (b) Comparison of fluorescent intensity of the microarrays features on glass and alkyne-HEMA-EDMA substrates after incubation with different concentrations of antibodies.

3-Dimensional microarrays are created in a nanoporous polymer film. The microarrays are stabilized by covalent attachment over a click-chemistry approach and exhibit an enhanced dynamic range for the detection of antibody binding due to a higher amount of binding sites in the nanoporous film compared to flat substrates with conventional 2-dimensional surface arrays.

3D Microarrays

M. Hirtz*, W. Feng, H. Fuchs, and P. A. Levkin*

Click-Chemistry Immobilized 3D-infused Microarrays in Nanoporous Polymer Substrates